[9] M. Kretowski, Y. Rolland, J. Bezy-Wendling, and J. Coatrieux, "Fast algorithm for 3-D vascular tree modeling," *Comput. Meth. Prog. Biol.*, vol. 70, no. 2, pp. 129–136, 2003.
[10] K. Bae, J. Heiken, and J. Brink, "Aortic and hepatic contrast medium enhancement at CT, prediction with a computer model," *Radiology*, vol. 207, pp. 647–655, 1998.
[11] S. Kim, J. Kim, J. Han, K. Lee, and B. Min, "Prediction of optimal injection protocol for tumor detection in contrast-enhanced dynamic hepatic CT using simulation of lesion to liver contrast difference," *Comput. Med. Imag. Graphics*, vol. 24, pp. 317–327, 2000.
[12] G. Brix *et al.*, "Regional blood flow, capillary permeability, and compartmental volumes: Measurement with dynamic CT—Initial experience," *Radiology*, vol. 210, pp. 269–276, 1999.
[13] E. Carson and C. Cobelli, *Modelling Methodology for Physiology and Medicine*. New York: Academic, 2001.
[14] C. Chapple *et al.*, "A model of human microvascular exchange: Parameter estimation based on normals and nephrotics," *Comput. Meth. Prog. Biol.*, vol. 41, pp. 33–54, 1993.
[15] B. Fagrell, "Advances in microcirculation network evaluation: An update," *J. Microcirc.*, vol. 15, pp. 34–40, 1995.

Cancellation of Ventricular Activity in the ECG: Evaluation of Novel and Existing Methods

Mathieu Lemay*, Jean-Marc Vesin, Adriaan van Oosterom, Vincent Jacquemet, and Lukas Kappenberger

***Abstract*—Due to the much higher amplitude of the electrical activity of the ventricles in the surface electrocardiogram (ECG), its cancellation is crucial for the analysis and characterization of atrial fibrillation. In this paper, two different methods are proposed for this cancellation. The first one is an average beat subtraction type of method. Two sets of templates are created: one set for the ventricular depolarization waves and one for the ventricular repolarization waves. Next, spatial optimization (rotation and amplitude scaling) is applied to the QRS templates. The second method is a single beat method that cancels the ventricular involvement in each cardiac cycle in an independent manner. The estimation and cancellation of the ventricular repolarization is based on the concept of dominant T and U waves. Subsequently, the atrial activities during the ventricular depolarization intervals are estimated by a weighted sum of sinusoids observed in the cleaned up segments. ECG signals generated by a biophysical model as well as clinical ECG signals are used to evaluate the performance of the proposed methods in comparison to two standard ABS-based methods.**

***Index Terms*—Atrial fibrillation, average beat subtraction, ECG preprocessing, QRST cancellation.**

I. Introduction

Atrial fibrillation (AF) is the most common type of human cardiac arrhythmia. The diagnosis of AF as such has been based mainly on visual inspection of the surface electrocardiogram (ECG) [1]. Due to the much higher amplitude of the electrical ventricular activity (VA) on the surface ECG, cancellation of the ventricular involvement is crucial in the study of AF on ECGs. Two approaches are generally used to perform this task: source separation algorithms and matched template subtraction. Source separation algorithms try to find uncorrelated components using a principal component analysis (PCA), or to find independent components in an instantaneous linear mixture using an independent componant analysis (ICA). PCA have previously been employed to monitor the effects of drugs [2] and assess the effects of linear left atrial ablation [3]. ICA has been applied in order to obtain ECG signals devoid of VA involvement [4] and [5]. In these algorithms, even if the obtained components do not seem to contain any VA involvement, they are not anymore associated to specific locations on the thorax.

Other well-known methods are based on the subtraction of matched templates. These methods assume that, in the same patient, ventricular complexes generally exhibit a limited number of forms. An average (template) of these distinct complexes is then used to subtract the VA. In this paper, the standard average beat subtraction (ABS) method (without any features) is labelled as ABS_1. Studies of noninvasive assesment of the atrial cycle length [6], frequency analysis of AF and drugs effects [7] and classification of paroxysmal and persistent AF [8] are some of the numerous examples in which matching template and subtraction methods were used to cancel ventricular involvement. A refined method was described by Stridh and Sörnmo [9], labelled here as ABS_2. In their method, two major features are added: F wave reduction and spatiotemporal alignment. In this method, several beats for each morphology are needed to create the templates. In clinical practice, the standard ECG consists of 10-s recordings, and high quality templates may be difficult to create.

In this paper, we propose two methods for ventricular wave suppression. The first one is a further refinement of ABS_1, labelled as ABS_3, and as such can be applied only if a sufficiently long episode of AF in the ECG signal is available. The second is a method that permits cancellation of the ventricular involvement in short episodes of AF in the ECG signal, with a minimum length of one complete cardiac cycle. This method is labelled as single beat (SB). Both the ABS_3 and the SB treat the ventricular depolarization (QRS complexes) and repolarization (T and U waves) separately. A dedicated preprocessing procedure is presented in Section II. The two main steps of ABS_3 are explained in Section III: QRS complex cancellation using templates (Section III-A) and T and U wave cancellation using templates (Section III-B). The two main steps of the SB method are presented in Section IV: cancellation during the JQ intervals using dominant T and U wave approach (Section IV-A) and estimation of AA during the QRS intervals using a weighted sum of sinusoids (Section IV-B). The performances of the two methods are studied in their application to ECG signals generated by a biophysical model of the atria, as well as to clinical recordings (see Section V). By using the model, realistic separate contributions of the atria and the ventricles became available for testing the methods. The performances of the two methods are compared to those of the standard ABS method without (ABS_1) and with (ABS_2) spatiotemporal alignment, as was proposed in [9].

II. Preprocessing

In the standard 12-lead ECG, only two of the first six leads (I, II, III, VR, VL, and VF) are linearly independent. This justified the expression of the pertinent information by an T-by-8 matrix $\mathbf{X}$ that comprises T samples from eight leads: two limb leads (VR and VL) and six precordial leads (V1 to V6). A derivative-based method was applied to the root mean square (rms) signal to detect ventricular complexes [10]. In the ith

Manuscript received February 13, 2006; revised August 20, 2006. This work was supported in part by the Theo-Rossi-Di-Montelera Foundation and in part by the Swiss National Science Foundation (SNSF). *Asterisk indicates corresponding author.*

*M. Lemay is with Ecole Polytechnique Fédérale de Lausanne (EPFL), Signal Processing Institute, Lausanne CH-1015, Switzerland. (e-mail: mathieu.lemay@epfl.ch).

J.-M. Vesin and V. Jacquemet are with the Ecole Polytechnique Fédérale de Lausanne (EPFL), Signal Processing Institute, Lausanne CH-1015, Switzerland.

A. van Oosterom, and is with the Department of Cardiology, CHUV, Lausanne CH-1015, Switzerland.

L. Kappenberger is with Cardiomet, CHUV, Lausanne CH-1015, Switzerland.

Digital Object Identifier 10.1109/TBME.2006.888835

cardiac cycle, the timing of the onset of the ventricular depolarization was denoted as q_i, where the index i refers to the ith cardiac cycle. The R wave timing, denoted as r_i, was defined as the middle point between the closest samples on either side, below 50% of the maximum value of the rms curve. The J point timing, denoted as j_i, was defined as the local minimum of the rms curve between r_i and the timing of the subsequent T wave peak. This T wave peak timing on the rms curve was denoted as k_i.

A baseline correction was applied to each of the eight lead signals by means of a cubic spline interpolation anchored on the onset points q_i identified in the rms signal [11]. The fiducial point detection and the baseline correction were iteratively applied until no further changes in their timing were observed. The eight resulting ECG signals were smoothed by applying a low-pass finite impulse response filter (moving average window of 20 ms).

III. Method Based on Matching Template and Subtraction

As previously suggested by Waktare *et al.*[12], our method treats the QRS complexes and JQ intervals (extended ST-T intervals) separately. The ith QRS complex was represented by an L_i-by-8 matrix $\mathbf{A}_i$ containing the samples between q_i and j_i. The ith JQ interval was represented by an M_i-by-8 matrix $\mathbf{B}_i$ containing the samples between j_i and q_{i+1}. The whole cardiac cycle was represented by an N_i-by-8 matrix $\mathbf{C}_i$ containing the samples between q_i and q_{i+1}. Averages of similar QRS complexes $\mathbf{A}_i$ or JQ intervals $\mathbf{B}_i$ were used as templates.

A. Ventricular Activity Cancellation During the QRS Intervals

The QRS complexes were clustered based on the morphology of the eight lead signals. In order to compare the morphology of the QRS complex $\mathbf{A}_i$ and $\mathbf{A}_j$, the normalized zero-delay cross-correlation between the corresponding columns (leads) of the two matrices aligned with r_i and r_j was computed. The matrices were considered similar if all eight correlation values were above a given threshold (θ).

The QRS complexes within the kth cluster Ω_k were aligned using their R wave timings (r_i). The individual QRS complexes within any cluster Ω_k were permitted to be of different lengths. The template $\mathbf{T}_k$ was defined as the sample-wise average of the QRS complexes composing Ω_k: the averaging at each time index was carried out only if more than one sample was available at that time index. If not, the values of the row of template $\mathbf{T}_k$ at that time index were set to zero.

Each template $\mathbf{T}_k$ was temporally aligned with the R wave timings for all QRS complexes assigned to cluster Ω_k. A template $\widetilde{\mathbf{T}}_i$ was obtained by applying a spatial optimization (rotation and independent scaling) to the QRS templates $\mathbf{T}_k$ to compensate possible variations in the electrical axis, tissue conductivity and heart position, [9]. The final estimate of the atrial activity inside the complex $\mathbf{A}_i$ was taken to be the residual difference $\mathbf{A}_i - \widetilde{\mathbf{T}}_i$. In contrast to [9], the QRS complex cancellation method used the same timings as were used during template creation to realign the templates before the spatial optimization.

B. Ventricular Activity Cancellation During the JQ Intervals

There were three differences between the algorithms used for treating either the QRS complex or the JQ interval. The first relates to the fact that the normalized zero-delay cross-correlation values used for the comparison were measured on the rms curves related to different beats $\mathbf{B}_i$ and $\mathbf{B}_j$. The second was the timing used for the JQ interval and template alignment. These timings were defined at a fixed distance following the R wave timings r_i. This distance was the average distance between all T wave timings k_i and their preceding R wave timings r_i. In the same way as described in Section III-A, a template $\mathbf{T}_z$ was built for each JQ cluster Ω_z using the same sample-wise average approach. The third was that no spatial optimization was applied to the JQ interval templates $\mathbf{T}_z$. The estimate of AA inside $\mathbf{B}_i$ was taken to be the difference $\mathbf{B}_i - \mathbf{T}_z$, with $\mathbf{T}_z$ the JQ interval template corresponding to $\mathbf{B}_i$.

A zero-phase fifth-order Butterworth filter with a cutoff frequency of 50 Hz was applied after the cancellation to smooth any remaining discontinuity between each QRS complex and the subsequent JQ interval. Leads I, II, III, and VF were recaptured by the appropriate linear combination of leads VR and VL.

IV. Cancellation Method Applicable to Single Beats

In contrast with the ABS methods, our SB method treats each cardiac cycle independently. First, the JQ intervals were processed by using a dominant wave approach. Then, AA located in the QRS intervals was estimated by a finite sum of sinusoids by using the estimated AA (after T and U cancellation) in the neighboring JQ intervals.

A. Ventricular Activity Cancellation During the JQ Intervals

The shapes of the T waves as observed in different leads placed on the thorax are very similar. The dominant T wave, $T_{\mathrm{dom}}(t)$, has been introduced as a means to characterize this general signal shape [13]. It was estimated by the first principal component over the ST-T interval

$$\boldsymbol{T}_{\mathbf{dom}} = \mathbf{e}^T \boldsymbol{\Phi}^T \tag{1}$$

where the V-by-8 matrix $\boldsymbol{\Phi}$ represents the ECG lead signals during the ST-T interval, the 8-vector $\mathbf{e}$ represents the first eigenvector (associated with the highest eigenvalue) of the estimated covariance matrix of $\boldsymbol{\Phi}$, and $\boldsymbol{T}_{\mathbf{dom}}$ represents $T_{\mathrm{dom}}(t)$ over the ST-T interval. Since this method uses information within the individual beat only, here the index i will be dropped.

Based on a biophysical model of the genesis of the T wave, it was shown that an individual T wave could be represented by a linear combination of the function $T_{\mathrm{dom}}(t)$ and its time derivatives [14]. In an application to clinical ECGs it was found that taking third-order derivatives generally resulted in components that could hardly be distinguished from noise. In the current application, derivatives up to the second-order only were included. Before taking its derivative, $T_{\mathrm{dom}}(t)$ was fitted with a smooth analytical function. The function used was the product of two logistic functions [15]

$$f(t) = p_1 \left(p_2 + \frac{1}{1 + e^{p_3(t-p_5)}} \cdot \frac{1}{1 + e^{p_4(t-p_5)}} \right) \tag{2}$$

where p_1 is an overall scaling factor, p_2 sets the initial value, p_3 and p_4 are parameters for the positive and negative slope, and p_5 sets the timing of the apex of the dominant T wave. In the ECGs of most AF patients, U waves were observed. The shape of the observed U waves was similar to that of a Gaussian function. Correspondingly, the general, dominant shape of the U wave was expressed as

$$g(t) = p_6 \, e^{-[(t-p_8)/p_7]^2} \tag{3}$$

where p_6 is an overall scaling factor of U wave amplitude, p_7 its width, and p_8 the timing of its apex.

The cancellation applicable to SBs was based on the two dominant functions $f(t)$ and $g(t)$. The eight parameters involved were found by fitting the function $f(t) + g(t)$ to $T_{\mathrm{dom}}(t)$. A nonlinear parameter estimation method needed to be used, for which we took the Levenberg–Marquart algorithm [16].

In the final step, a linear combination of the functions $f(t)$, $f'(t)$, $f''(t)$, and $g(t)$ was fitted to the observed data matrix $\mathbf{B}$. This constitutes a linear parameter estimation problem and, hence, the 4-by-8 matrix $\mathbf{W}$ representing the linear weights for the individual leads was computed as

$$\mathbf{W} = (\mathbf{U}^T\mathbf{U})^{-1}\mathbf{U}^T\mathbf{B} \tag{4}$$

in which the columns of matrix $\mathbf{U}$ are the functions $f(t)$, $f'(t)$, $f''(t)$, and $g(t)$ over $\mathbf{B}$. The estimate of AA was taken as $\mathbf{B} - \mathbf{UW}$.

B. Atrial Activity Estimation During the QRS Intervals

The cancellation of the ventricular involvement in the JQ intervals B_{i-1} and B_i produces a time interval of length $(M_{i-1} + L_i + M_i)$ in which the ventricular involvement in the QRS interval A_i remains to be treated. Rather than using a cancellation method, the atrial components in segments A_i were estimated from the AA observed in the cleaned up segments B_{i-1} and B_i.

The approach assumes that AA signals are stationary over one cardiac cycle. Frequency analysis of AF signals free of ventricular involvement has demonstrated a narrow band in the frequency domain. This led us to express the AA signal over the QRS intervals A_i of a single lead as finite sum of sinusoids

$$s(t) = \sum_{k=1}^{P} s_k(t) = \sum_{k=1}^{P} \alpha_k \cos(2\pi f_k t) + \beta_k \sin(2\pi f_k t). \quad (5)$$

Applied to the complete set of leads, this expression reads

$$\mathbf{A}_i = \mathbf{S}_i \mathbf{E}_i \quad (6)$$

in which the columns of the L_i-by-2P matrix $\mathbf{S}_i$ are the P cosine and P sine functions during the interval A_i and the columns of the 2P-by-8 coefficient matrix $\mathbf{E}_i$ are the P parameters α_k and β_k for each lead. The frequency f_k of the P cosine and P sinus functions was uniformly distributed at P values between 0 and 10 Hz. The matrix $\mathbf{E}_i$ was computed as

$$\mathbf{E}_i = \mathbf{S}_i^{\dagger} \mathbf{B}_i^{C} \quad (7)$$

where $\mathbf{S}_i^{\dagger}$ is the pseudoinverse of $\mathbf{S}_i^{C}$ that contains the P cosine and P sinus functions during the intervals B_{i-1} and B_i, and $\mathbf{B}_i^{C}$ is the concatenation of the JQ matrices $\mathbf{B}_{i-1}$ and $\mathbf{B}_i$.

As in the first method, a low-pass Butterworth filter was applied at the end of this process and leads I, II, III, and VF were recaptured as the appropriate combination of leads VR and VL in the first method.

V. Database

A. Synthetic Signals

A 3-D model of the human atria was constructed from magnetic resonance (MR) images, including the openings at the sites of the entries and exits of the vessels as well as at the locations of the valves connecting the atria to the ventricles [17]. In order to create substrates for AF, patchy heterogeneities in action potential duration were introduced by modifying the local membrane properties. Simulated AFs induced by rapid pacing in the left atrium appendage were observed as multiple reentrant wave fronts that propagate and interact in a random fashion over the atrial surface. Nine different simulated AF types, ranging from 11.3 to 23.9 s, were created by modifying the pacing protocol and the heterogeneities.

Body surface potentials associated with the AA were computed by using a compartmental torso model including the atria, the ventricles, blood cavities and the lungs was constructed from MR images [18]. The nine ECG episodes of simulated AF were duplicated to cover 5 min. These nine 5-min ECGs of simulated AA were combined with two different clinical 5-min standard 12-lead ECGs of patients in sinus rhythm, from which the P waves were removed. In this manner, 18 realistic simulated 5-min AF signals sampled at 500 Hz were created in the standard 12-lead ECG.

B. Clinical Signals

Clinical database was used, composed of 180 5-min standard ECGs of patients in sustained AF. These signals were recorded and stored using a commercial recording system (CardioLaptop® AT-110, SCHILLER). The system used electrocardiographic filtering (0.05 to 150 Hz), a dynamic range of ± 10 mV AC (resolution of 5 μV) and a sampling rate of 500 Hz.

TABLE I
NORMALIZED mse OF THE QRS INTERVALS FOR EACH LEAD OF THE 18 SIMULATED ECGS

MSE	ABS_1	ABS_2	ABS_3	SB
VR	1.58 ± 1.45	1.36 ± 0.22	1.31 ± 0.19	1.12 ± 0.09
VL	1.90 ± 1.19	1.63 ± 0.40	1.43 ± 0.22	1.28 ± 0.17
V1	1.06 ± 0.36	1.01 ± 0.09	1.09 ± 0.19	1.13 ± 0.12
V2	1.96 ± 0.82	1.06 ± 0.25	1.17 ± 0.22	1.17 ± 0.09
V3	4.16 ± 3.58	1.22 ± 0.45	1.46 ± 0.54	1.14 ± 0.11
V4	6.08 ± 7.79	1.33 ± 0.73	1.41 ± 0.60	1.16 ± 0.17
V5	4.33 ± 3.90	1.26 ± 0.41	1.30 ± 0.36	1.18 ± 0.14
V6	2.82 ± 1.67	1.43 ± 0.24	1.32 ± 0.23	1.13 ± 0.12
Avg	**2.99 ± 2.60**	**1.29 ± 0.35**	**1.31 ± 0.32**	**1.16 ± 0.12**

TABLE II
NORMALIZED mse OF THE JQ INTERVALS FOR EACH LEAD OF THE 18 SIMULATED ECGS

MSE	ABS_1	ABS_2	ABS_3	SB
VR	0.30 ± 0.21	0.44 ± 0.20	0.16 ± 0.04	0.60 ± 0.28
VL	0.35 ± 0.21	0.52 ± 0.24	0.27 ± 0.12	1.08 ± 0.91
V1	0.27 ± 0.23	0.32 ± 0.21	0.12 ± 0.04	0.45 ± 0.10
V2	0.31 ± 0.22	0.33 ± 0.22	0.16 ± 0.04	0.80 ± 0.22
V3	0.35 ± 0.24	0.32 ± 0.21	0.22 ± 0.13	0.62 ± 0.21
V4	0.32 ± 0.24	0.33 ± 0.19	0.20 ± 0.15	0.61 ± 0.35
V5	0.31 ± 0.21	0.38 ± 0.21	0.16 ± 0.07	0.48 ± 0.15
V6	0.35 ± 0.21	0.50 ± 0.22	0.18 ± 0.06	0.55 ± 0.11
Avg	**0.32 ± 0.22**	**0.39 ± 0.21**	**0.18 ± 0.08**	**0.65 ± 0.29**

VI. Evaluation Procedure

The normalized mean square error (mse) between the original and the estimated AA was used to evaluate the simulated performance of the proposed ABS method (ABS_3) and the SB methods on all leads. The results were compared to those using the ABS_1 and the ABS_2 methods, as proposed in [9]. The algorithms used were based on the details mentioned in the respective literature. The thresholds (see Section III-A) were selected by analyzing the evolution of class numbers with respect to their values. The thresholds were selected as the values that correspond to the point just before the class numbers rapidly increase. For the ABS_3 method, the value of threshold for the QRS complexes (JQ intervals) was 0.93 (0.76, respectively). The threshold for ABS_1 and ABS_2 was fixed to 0.69. In the SB method, the parameter P was fixed at 50. This value resulted in a good balance between estimation error and over-fitting of the matrices $\mathbf{B}_{i-1}$ and $\mathbf{B}_i$.

A fifth-order high-pass Butterworth filter with a cutoff frequency of 1 Hz was applied bidirectionally to the resulting signals for all methods to remove any remaining frequency components below the physiological range. The normalized mse was evaluated for the QRS complex locations A_i and for the locations of all JQ intervals B_i separately.

Tables I and II summarize the performance of the various methods for the 18 simulated ECGs. On the 9th row, the average of all normalized mses for each method are indicated. Fig. 1 shows the results obtained by the two proposed methods applied to a 10-s segment.

The performance of the two proposed methods was also tested on clinical data. In these signals, the real AA on the ECG was obviously unknown. The only evidence of the success of ventricular complex cancellation was the absence of clear QRS residues. The testing was carried out as follows for each lead.

1) The interquartile range (qr) and the median (m) values of the amplitude distribution of the estimated AA signals was captured for the four methods: ABS_1, ABS_2, ABS_3, and SB.
2) The standard deviation (σ) was estimated from qr, as $\sigma = qr/0.6745$, the denominator corresponding to the value pertaining to the normal distribution. This way of estimating σ was used to eliminate the impact of outliers.

Fig. 1. (a) ECG from a 76-year-old patient in sinus rhythm, $\boldsymbol{P}$ wave removed. (b) ECG signal obtained by the addition of (c) AA and (a) VA ECG signal. (c) Original 10-s ECG simulated AA on VR. (d) Estimated AA with the $\mathbf{ABS}_3$ method after applying a high-pass filter with a cutoff frequency of 1 Hz. (e) Estimated AA with the SB method after applying the same high-pass filter. (f) Original AA of (c) amplified four times. (g) Estimated AA of (d) amplified four times; QRS mse of 0.25 and JQ mse of 0.08. (h) Estimated AA of (c) amplified four times; QRS mse of 0.53 and JQ mse of 0.47.

TABLE III
PERCENTAGE OF SIGNIFICANT QRS RESIDUES DETECTED ON 180 CLINICAL 5-MIN ECG RESULTS. THIS PERCENTAGE IS CALCULATED FOR EACH LEAD

% of QRS	ABS_1	ABS_2	ABS_3	SB
VR	33.5 %	15.4 %	5.8 %	3.4 %
VL	44.6 %	16.4 %	6.8 %	5.5 %
V1	34.0 %	11.3 %	4.6 %	3.1 %
V2	59.4 %	23.7 %	12.2 %	4.8 %
V3	59.0 %	23.0 %	12.4 %	2.7 %
V4	58.7 %	24.5 %	14.2 %	3.7 %
V5	55.4 %	22.0 %	12.3 %	3.5 %
V6	50.9 %	18.3 %	8.8 %	4.2 %
Average	**53.8 %**	**21.0 %**	**12.0 %**	**3.9 %**

3) The QRS complex intervals that contained absolute values above the threshold ς were identified, where $\varsigma = m + 2\sigma$. The QRS complex residues in these intervals were defined as being significant.

Table III shows the percentage of QRS complexes that were imperfectly cancelled. The ninth row represents the average percentage for each method.

When tested on the simulated signals, it was observed that this validation threshold ς detected less than 1% of all QRS intervals as significant QRS residues for each of the four methods.

VII. DISCUSSION

For any ventricular wave cancellation study, the major problem is the validation and the optimization of the different parameters. In this study, a biophysical model of the atria provided realistic ECG signals during AF to which clinical ventricular components were added. The latter were used to validate the approach based on separate ventricular depolarization and repolarization templates and to analyze the effect of the spatial optimization on the QRS complexes and on the T and U waves which led to the refined version of the standard ABS methods (ABS_3). The simulated ECG signals were also used to optimize the dominant wave approach (number of derivatives, T and U wave functions, etc.) and the estimation of the AA located in the QRS complexes (observations on the AA signal properties, number of sinusoids, etc.) that led to the SB cancellation method.

The major limitation of the ABS method is the need for long ECG signals with regular VA complexes of the same type, including extrasystoles. The other limitation of ABS-based methods is the imprecision in the cancellation of the QRST complexes. The cancellation during the QRS interval was much worse than during the JQ intervals, see Table I compared to Table II. A limitation of the SB method is the use of the first principal component to obtain the T and U wave estimates. In some cases, the correlation between AA and VA is too high, the first principal component will contain AA. Some of it will be removed by the analytical fitting step, but in a few patients, some AA components are included in $f(t)$ and the analytical fitting and further steps will include this error.

It was important to analyze the effects of the separate cancellation of ventricular depolarization and repolarization and the effect of the spatial optimization on the templates. Results on simulated signals show that the performance improved by this separate approach in ABS_3 as compared to the ABS-based methods that treat QRS complexes and T and U waves together (ABS_1 and ABS_2 [9]) (Tables I and II). We attribute this amelioration to three factors. The first is related to the physiological origin of ventricular waves. It may happen that repolarization waves are of different natures even if their respective depolarization waves are not. The second is that the morphologies of repolarization and depolarization waves are different. The VA templates are more accurate if they come from separate depolarization and repolarization wave clusters. These two factors may explain why the ABS_3 method obtains better cancellation results in the JQ intervals than the standard ABS-based method without template modifications (ABS_1), see first and third columns of Table II; for the JQ intervals, the only difference between these two methods are their clusters. The third is related to the criteria used for template modification; modification by rotation and scaling of the ventricular templates is beneficial for the QRS complexes but not for the JQ intervals. The minimization of the Frobenius norm between the ventricular templates and the original complexes produces efficient results on the QRS complexes because, in the QRS intervals, the amplitude and the frequency contents of VA are greatly different to the ones related to AA. This explains the excellent results for both ABS-based methods that apply these modifications to the QRS complex templates (ABS_2 and ABS_3), see columns 2 and 3 of Table I. However, it is not the case in the JQ intervals. The minimization of the Frobenius norm does not properly modify the JQ interval templates. This may explain why the ABS_1 method obtains better cancellation results in the JQ intervals than the ABS_2, see first and second columns of Table II; for the JQ intervals, the only difference between ABS_1 and ABS_2 is that the ABS_1 method does not modified the JQ interval templates. This justifies refraining from spatial optimization applied to the JQ interval templates, as was the case in ABS_3.

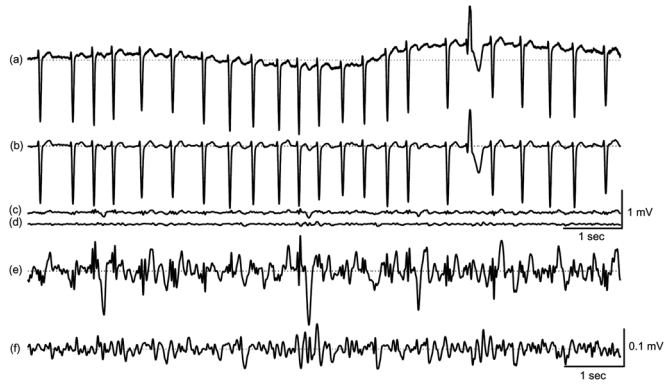

Fig. 2. (a) Clinical 10-s ECG signal on V2. (b) Clinical 10-s ECG signal after preprocessing. (c) Estimated AA with the $\mathbf{ABS}_3$ method after applying the high-pass filter with a cutoff frequency of 1 Hz. (d) Estimated AA with our SB method after applying the same high-pass filter. (e) Estimated AA of (c) amplified ten times; the third and eleventh QRS complexes residue remain clearly visible in this 10-s segment. (f) Estimated AA of (d) amplified ten times; no QRS complex residue was clearly visible in this 10-s segment.

The simulated results shown in Fig. 1 demonstrate the high quality of the ABS_3 method with a separate approach for the QRS complexes and the T and U waves. The SB method produces good results. Typical QRS artefacts are present in 2th and 6th QRS complexes in the ABS_3 result, but not in the result of SB. In the validations on simulated signals, the normalized mse values were used to evaluate the cancellation performance. Usually, the QRS residues are larger than T and U wave residues (average of all normalized mse of 1.68 for QRS and 0.39 for T and U). These QRS residues are characterized by a wide frequency band and, therefore, have a stronger impact on the estimated spectrum of the AA, for example. They are regularly present in clinical cancellation results obtained by ABS methods where the ventricular complexes are not as regular as during sinus rhythm. This is also why the SB method may still be of interest even if its performance on simulated signals is lower than others for the T and U waves.

Table III shows that the SB-based method contains fewer detected QRS complex residues than the other ABS-based methods. This is related to the smoothness of the AA estimates in QRS intervals. In terms of visual validation and frequency contents, these AA estimates look more natural than the typical noisy intervals obtained by an ABS method. We can also see that modification of the ventricular templates and the separate approaches for QRS complexes and T and U waves reduce the number of episodes showing significant residues. For the AF signal obtained by ABS_3 shown in Fig. 2(e), the QRS residues in the 3rd and 11th QRS complex intervals were considered significant, but typical ABS-based method residues are also visible within the other QRS and T wave intervals. These residues do not show up in the typical SB result shown in Fig. 2(f).

The clinical results demonstrate that the local estimation of the AA produces significantly smaller QRS complex residues than the cancellation methods based on subtraction. The AA estimation method is efficient because it involves the estimation of relatively short segments (QRS intervals), while using the local information on longer AA segments (JQ intervals). The latter are made available by the cancellation of ventricular repolarization waves using the dominant wave approach.

VIII. Conclusion

Two different methods are proposed to cancel the ventricular involvement in the standard 12-lead ECG with high quality results. In the situation where the ventricular complexes are highly regular and where the ECG record contains a sufficient number of ventricular complexes, the use of the proposed ABS-based method (ABS_3) is appropriate. In the situation where ventricular complex morphology is variable, which is the case in most AF patients, or when the ECG record contains few ventricular complexes, the use of the proposed SB method is to be preferred and produces accurate results.

Acknowledgment

The authors would like to thank A. Forclaz who heads a specific project that made this study possible. They would also like to thank V. Prudent who is in charge of the clinical database.

References

[1] V. Fuster *et al.*, "ACC/AHA/ESC guidelines for the management of patients with atrial fibrillation: Executive summary: A report of the American College of Cardiology/American Heart Association Task Force on Practice Guidelines and the European Society of Cardiology Committee for Practice Guidelines and Policy Conferences," *J. Am. Coll. Cardiol.*, vol. 38, no. 4, pp. 1231–1265, 2001.

[2] D. Raine, P. Langley, A. Murrray, A. Dunuwille, and J. P. Bourke, "Surface atrial frequency analysis in patients with atrial fibrillation," *J. Cardiovasc. Electrophysiol.*, vol. 15, pp. 1021–1026, 2004.

[3] D. Raine, P. Langley, A. Murrray, S. S. Furniss, and J. P. Bourke, "Surface atrial frequency analysis in patients with atrial fibrillation: Assessing the effects of linear left atrial abalation," *J. Cardiovasc. Electrophysiol.*, vol. 16, pp. 838–844, 2005.

[4] M. Lemay, J. M. Vesin, Z. Ihara, and L. Kappenberger, "Suppression of ventricular activity in the surface electrocardiogram of atrial fibrillation," in *Proc. ICA 2004*, 2004, pp. 1095–1102.

[5] F. Castells, J. J. Rieta, J. Millet, and V. Zarzoso, "Spatiotemporal blind source separation approach to atrial activity estimation in atrial tachyarrhythmias," *IEEE Trans. Biomed. Eng.*, vol. 52, no. 2, pp. 258–267, Feb. 2005.

[6] M. Holm, S. Pehrson, M. Ingemansson, L. Sornmo, R. Johansson, L. Sandhall, M. Sunemark, B. Smideberg, C. Olsson, and S. B. Olsson, "Non-invasive assesment of the atrial cycle length during atrial fibrillation in man: Introducing, validation and illustrating a new ECG method," *Cardiovasc. Res.*, vol. 38, pp. 69–81, 1998.

[7] A. Bollmann, N. K. Kanuru, K. K. McTeague, P. F. Walter, D. B. DeLurgio, and J. J. Langberg, "Frequency analysis of human atrial fibrillation using the surface electrocardiogram and its response to ibutilide," *Am. J. Cardiol.*, vol. 81, pp. 1439–1445, 1998.

[8] A. Bollmann, K. Sonne, E. H. D. I. Toepffer, J. J. Langberg, and H. U. Klein, "Non-invasive assesment of fibrillatory activity in patients with paroxysmal and persistent atrial fibrillation using the holter ECG," *Cardiovasc. Res.*, vol. 44, pp. 60–66, 1999.

[9] M. Stridh and L. Sörnmo, "Spatiotemporal QRST cancellation techniques for analysis of atrial fibrillation," *IEEE Trans. Biomed. Eng.*, vol. 48, no. 1, pp. 105–111, Jan. 2001.

[10] Z. Ihara, A. van Oosterom, and R. Hoekema, "Atrial repolarization as observable during the pq interval," *J. Electrocardiol.*, vol. 39, no. 3, pp. 290–297, 2006.

[11] L. Sörnmo and P. Laguna, *Bioelectrical Signal Processing in Cardiac and Neurological Applications*. Amsterdam, The Netherlands: Elsevier, 2005.

[12] J. Waktare, K. Hnatkova, C. Meurling, H. Nagayoshi, T. Janota, A. Camm, and M. Malik, *Optimal Lead Configuration in the Detection and Subtraction of QRS and* $\boldsymbol{T}$ *Wave Templates in Atrial Fibrillation*, ser. Computers in Cardiology. Berlin, Germany: Springer-Verlag, 1998, vol. 25, pp. 629–632.

[13] A. van Oosterom, "The dominant $\boldsymbol{T}$ wave and its significance," *J. Cardiovasc. Electrophysiol.*, vol. 14, no. 10, pp. S180–S187, 2003.

[14] ——, "Singular value decomposition of the $\boldsymbol{T}$ wave: Its link with a biophysical model of repolarization," *Int. J. Bioelectromagnetism*, vol. 4, pp. 59–59, 2003.

[15] A. van Oosterom and V. Jacquemet, "A parametrized description of transmembrane potential used in forward and inverse procedures," *Folia Cardiologica*, vol. 12, pp. 111–111, 2005.

[16] D. W. Marquart, "An algorithm for least-squares estimation of nonlinear parameters," *J. Soc. Ind. Appl. Math.*, vol. 2, pp. 431–441, 1963.

[17] V. Jacquemet, A. van Oosterom, J. M. Vesin, and L. Kappenberger, "A biophysical model approach to the analysis of electrocardiograms during atrial fibrillation," *IEEE Eng. Med. Biol. Mag.*, 2007, to be published.

[18] A. van Oosterom and V. Jacquemet, "Genesis of the $\boldsymbol{P}$ wave: Atrial signals as generated by the equivalent double layer source model," *Europace*, vol. 7, pp. S21–S29, 2005.